

Petrographical Characteristics of Ultramafic Xenoliths from Megata Volcano, the Northeast Japan Arc

メタデータ	言語: eng 出版者: 公開日: 2017-10-03 キーワード (Ja): キーワード (En): 作成者: 阿部, なつ江, 荒井, 章司 メールアドレス: 所属:
URL	https://doi.org/10.24517/00011167

This work is licensed under a Creative Commons Attribution-NonCommercial-ShareAlike 3.0 International License.



Petrographical characteristics of ultramafic xenoliths from Megata volcano, the Northeast Japan arc

Natsue ABE and Shoji ARAI

Department of Earth Sciences, Kanazawa University, Kanazawa 920-11, Japan

Abstract: Petrographical characteristics of ultramafic xenoliths from Megata volcano, Northeast Japan arc, are described to understand igneous and metasomatic processes within the mantle wedge. Petrographical variation in xenolith suite from Ichinomegata to Sannomegata through Ninomegata indicates a horizontal mantle heterogeneity in terms of degree of hydration and degree of refractoriness beneath the arc. Dunite, which is very small in abundance, occurs as thin layers or patches closely associated with pyroxenites or pyroxene-rich layers. It is a kind of depletion aureole around melt conduits. Chromitite is almost absent because of the averaged high fertility of the peridotite.

1. Introduction

Ultramafic xenoliths from the Megata volcano, Northeast Japan arc, are very important because they are derived from the mantle wedge of the arc. Peridotite xenoliths are usually brought up by alkaline basalts of intraplate type or by kimberlites and related magmas and, therefore, represent the upper mantle beneath oceanic hotspots, continental rifts and continental cratons. Arc magmas carrying mantle xenoliths are very rare on the

earth. Richard (1986) and Vidal et al. (1985) reported partly metasomatized peridotite xenoliths in calc-alkaline andesite from Batan island, the Philippines. Ninomiya and Arai (1992) found harzburgite fragments in gabbroic xenoliths from andesite of the Oshima-Ōshima volcano, northern Japan. Peridotite xenoliths have been found in arc magmas of Mt. Verbyud, Kamchatka, Russia (S. Shcheka, personal com. 1993).

In this article we would like to describe petrographical characteristics of the Megata ultramafic xenoliths in order to understand mantle processes beneath the arc. We especially focus on relationships between different rock types on so-called composite xenoliths. The studies ever

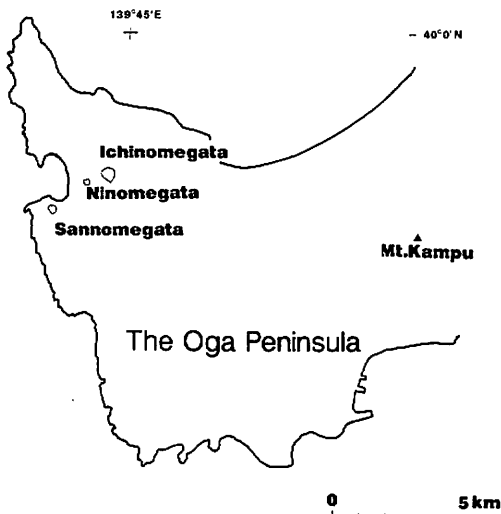


Fig. 1. Locality map of the Megata volcano, the Northeast Japan arc. Note that the distance from Ichinomegata to Sannomegata is approximately 2.5 km.

done on the Megata xenoliths have oriented to petrology, or more frequently, to geochemistry (e.g., Aoki and Prinz, 1974; Takahashi, 1980; Tanaka and Aoki, 1987), and detailed petrographical descriptions have not yet been done and are rather new.

The Megata volcano, located at the western end of the Oga Peninsula, has three craters, Ichinomegata, Ninomegata and Sannomegata (Fig. 1). Ichinomegata crater, erupting calc-alkaline andesite to dacite, is the oldest, ca.10,000 years in age (Horie, 1964), and the Sannomegata crater, erupting high-alumina basalt, is the youngest (Katsui et al., 1979). Petrological characteristics of the Ninomegata crater have not been clarified both for volcanics and xenoliths. Kampu volcano, erupting calc-alkaline andesite, alkaline basalt and high-alumina basalt with relatively high K, is located at the eastern part of the Oga Peninsula (Fig. 1). The main volcanic activity of the Kampu volcano initiated ca. 20,000 years ago, older than the Megata volcano (Fujinawa and Hayashi, 1993).

2. Petrography

2.1 Peridotite xenoliths

Peridotite xenoliths from Megata volcano are up to 30 cm, but usually less than 10 cm, in diameter. They are classified into three groups, lherzolite, harzburgite and dunite-wehrlite in terms of mode.

Lherzolite

Lherzolites are usually finer-grained (Plate I, fig. 1) than harzburgite (Plate II, figs. 1 & 2) and dunite-wehrlite (Plate XI, fig. 1). The fine-grained lherzolites are characterized by presence of the pyroxene-spinel symplectite, a fine-grained aggregate of vermicular green-spinel, clinopyroxene and orthopyroxene. (Plate VI, figs. 2 & 3), which may be formed by subsolidus reactions between olivine and plagioclase (Takahashi, 1986). Plagioclase has been sometimes preserved in the center of the symplectite. Lherzolites are composed mainly of olivine with subordinate amount of orthopyroxene; spinel and clinopyroxene are less in amount, usually < 5 vol.% and < 10 vol.%, respectively. Peridotite xenoliths from Sannomegata are almost lherzolite enriched with fine-grained aggregate, which may be a decomposition product of spinel-pyroxene symplectite. Secondary pargasite, usually less than 2 vol.%, commonly replaces pyroxene-spinel symplectite in lherzolites from Ichinomegata (Plate VI, figs. 2 & 3) and Ninomegata as mentioned later.

Harzburgite

Harzburgite is generally coarse-grained (Plate II) compared with lherzolite but is rarely finer-grained than lherzolite (Plate III). Clinopyroxene is rare, and spinel-pyroxene symplectite and plagioclase are totally absent. The fine-grained harzburgite characteristically has porphyroclastic texture; olivine and orthopyroxene porphyroclasts are strongly

deformed. Marginal parts of orthopyroxene porphyroclast and surrounding neoblasts of olivine and orthopyroxene are enriched with fine (dusty) chromian spinel inclusions (Plate III, Fig. 3). The coarse-grained harzburgite is almost equigranular. Orthopyroxene and clinopyroxene are usually full of chromian spinel lamellae. Orthopyroxene together with chromian spinel sometimes makes trails. Amphibole is rare in harzburgite (Abe et al., 1992).

Dunite and Wehrlite

Dunite and wehrlite are rather rare as xenoliths from the Megata volcano (Arai and Takahashi, 1987). Discrete dunite (or wehrlite) xenoliths are not so coarse-grained (e.g., Arai and Takahashi, 1987). Dunite and wehrlite often occur as small-scale layers and patches in other rocks. They are characteristically coarse-grained and are associated with pyroxenites or pyroxene-rich layers. Arai (1987) reported "olivine cumulates", which are mainly megacrystalline pyroxenites (or hornblendites) with various amounts of olivine chadacrysts.

2.2 Pyroxenite xenoliths

Pyroxenite xenoliths are common from Ichinomegata, occupying less than 10 % of whole xenoliths (Takahashi, 1986), and are less frequent than those from some xenolith localities of Southwest Japan arc (e.g., Arai and Kobayashi, 1981; Arai and Muraoka, 1992). From Ninomegata only one sample (clinopyroxenite) is found over 12 ultramafic xenoliths available. Pyroxenites from Sannomegata contain appreciable amounts (up to 53 %) of "fine-grained aggregate", which may be modified spinel-pyroxene symplectite (Saeki, 1979; Abe et al., 1992). Pyroxenites are coarser-grained than lherzolites but finer-grained than coarse-grained harzburgite.

Pyroxenites are variable from clinopyroxenite to websterite (or olivine websterite). Olivine clinopyroxenite (1 sample: Plate XI, Fig. 2) and orthopyroxenite (1 sample: Plate V, Fig. 4) are very rare. They have small amounts of chromian spinel and plagioclase. Opaque minerals (mainly sulfides) are rather abundant. There is a modal gap for plagioclase between gabbroic rocks and pyroxenites (Arai, 1990). Pyroxenes in all pyroxenites from Ichinomegata have numerous fluid inclusion trails with spinel and hydrous minerals (Plate IV, Fig. 1; Plate V, figs. 1 & 2). Amphibole is frequently formed at grain boundaries and sometimes occurs as veinlets cutting pyroxene grains (Plate V, Fig. 3).

We found only one pyroxenite sample from Ninomegata, which is clinopyroxenite. Amphibole is formed at grain boundaries but clinopyroxene is characteristically free from fluid inclusion trails (Plate IV, figs. 3 & 4).

2.3 Composite xenoliths

Various types of composite xenoliths have been found mainly in Ichinomegata. Composite xenoliths are especially important because we can know contact relationships of various rock types in the deep parts on them. Therefore, we would like to describe individual samples which we think important in this section.

Harzburgite with hornblendite selvages (I-706; Plate VII, figs. 1 & 2)

Harzburgite is mantled with thin hornblendite which has small amount of phlogopite. Very thin orthopyroxenite is present between harzburgite and hornblendite. Harzburgite has neither clinopyroxene nor amphibole. Orthopyroxene both from thin orthopyroxenite and harzburgite is enriched with minute spinel and other opaque inclusions. Abe et al. (1992) described this xenolith in detail. They interpreted that the hornblendite selvage was originally veinlets cutting the harzburgite in the upper mantle.

Lherzolite veined by hornblendite (N-05; Plate VII, figs. 3 & 4)

Lherzolite is cut by anastomosing veinlets of hornblendite. Hornblendite veinlets have many sulfide inclusions. The lherzolite is enriched with symplectites accompanied with pargasite. Color of the pargasite in lherzolite becomes deep towards the hornblendite veinlets, possibly indicating diffusion of volatiles from the hydrous melt which produced veinlets.

Hornblendite with peridotite selvage (I-933; Plate VIII)

The hornblendite, which is relatively fine-grained, has appreciable amount of plagioclases and orthopyroxene and is, therefore, partly gabbroic. The peridotite selvage is too thin to discriminate rock type, but may be lherzolite because spinel-pyroxene symplectite is preserved in and around the selvage (Plate VIII, Fig. 2). This rock could be originally either a hornblendite dike or a secondary hydrated gabbroic or websteritic dike in lherzolitic peridotite.

Pyroxene-rich lherzolite with websterite layer (I-883; Plate IX, figs. 1 & 2)

Websterite layer (or vein?) has coarse-grained dunite or pyroxene-poor peridotite layer on both sides. Amphibole is abundant in the websterite layer, mainly replacing clinopyroxene (Plate IX, Fig. 2). It is noteworthy that a dunite layer on one side (upper left of Fig. 1 of Plate IX) is extremely coarse-grained, of which olivine is up to 5 mm across.

Dunite vein in pyroxene-rich lherzolite (I-873; Plate IX, figs. 3 & 4)

Secondary amphibole is abundant in the pyroxene-rich lherzolite (or olivine websterite). The dunite is distinctively coarser-grained than the surrounding lherzolite.

Lherzolite veined by clinopyroxenite

(I-716, donated by H. Watanabe, University of Tsukuba; Plate X)

Clinopyroxenite vein has plagioclase in the center. It is noteworthy that symplectite and orthopyroxene in the lherzolite decreases in amount towards the pyroxenite vein. The lherzolite partly becomes dunitic adjacent to the vein. Dunitic patches are also present in the pyroxenite vein. Clinopyroxene in the vein is full of fluid inclusion trails similar to those in the discrete pyroxenite xenoliths from Ichinomegata.

Heterogeneous peridotite (I-738; Plate VI, figs. 3 & 4)

A relatively large (ca. 10 cm across) xenolith is patchy in lithology; modal amounts of pyroxenes and olivine varies appreciably in order of a few centimeters, from lherzolite to dunite through harzburgite. The lherzolitic part has spinel-pyroxene symplectite even near the dunitic part (Plate VI, Fig. 3). Amphibole is abundant, replacing spinel-pyroxene symplectite in the lherzolite part (Plate VI, Fig. 3) and clinopyroxene in the harzburgite part (Plate VI, Fig. 4).

Layered dunite, wehrlite and clinopyroxenite (I-734; Plate XI, Fig. 1)

Rocks are well layered and coarse-grained. Dunite is especially coarse-grained.

Websterite and gabbro with dunitic patch (I-745, Plate XI, figs. 3 & 4)

In gabbro, spinel-pyroxene symplectite is prominent between olivine and plagioclase. Pargasite replacing symplectite is formed along the boundary with olivine. Orthopyroxene is often formed between the symplectite (and/or pargasite) and olivine. In the gabbro, especially near the boundary between gabbro and websterite, some dunitic patches are present. Websterite is relatively enriched with pargasite replacing discrete clinopyroxene or clinopyroxene lamellae in orthopyroxene. The gabbro may have been initially troctolitic, because of the abundance of symplectite.

Wehrlite and websterite (I-765; Plate XI, Fig. 2)

Wehrlite and websterite share one xenolith (Plate XI, Fig. 2). Irregular-shaped dunitic patches are present in the wehrlite part (Plate XI, Fig. 2). The websterite part is abundant in inclusion trails (Plate XI, Fig. 2), which is hardly traceable, disappearing within a few grains of clinopyroxene, in the wehrlite part.

Lherzolite with orthopyroxene-rich layer

(I-735, Plate XII, figs. 1-3; I-777, Plate XII, Fig. 4)

Lherzolite is abundant in spinel-pyroxene symplectite in which plagioclase is still preserved. Secondary amphibole is frequently found. It is noteworthy that trails of tiny inclusions in orthopyroxene are traceable along the orthopyroxene-rich layer throughout the xenolith (Plate XII, Fig. 3).

2.4 Hydrous minerals

Presence of hydrous minerals is characteristic of some xenoliths from the Megata volcano, and may be very important to consider petrological evolution of the lower crust-upper mantle beneath the arc. The modes of occurrence hydrous minerals are reviewed in thin section.

Hydration is very common and sometimes very pervasive in both mafic and ultramafic xenoliths from Ichinomegata (e.g., Aoki, 1971; Takahashi, 1986) and Ninomegata (Abe and Arai, in prep). Sannomegata xenoliths are, however, very poor in hydrous minerals or their decomposition products (Arai and Saeki, 1981; Arai, 1990). Pargasite or pargasitic hornblende is the most common (e.g., Aoki and Shiba, 1973; Abe et al., 1992) and phlogopite is rarely found (Arai, 1986). Hydrous minerals are up to 20 vol. % and generally less than 2 vol. %.

In lherzolite, amphibole, which is pargasite or pargasitic hornblende, mainly replaces spine-pyroxene symplectite. Phlogopite is absent.

Hydrous minerals are generally rare in harzburgites. Two of harzburgite xenoliths are very rich in hydrous minerals (20 and 14 vol. %), which are the most hydrated ones of all peridotite xenoliths from the Megata volcano. Phlogopite is present only in such strongly

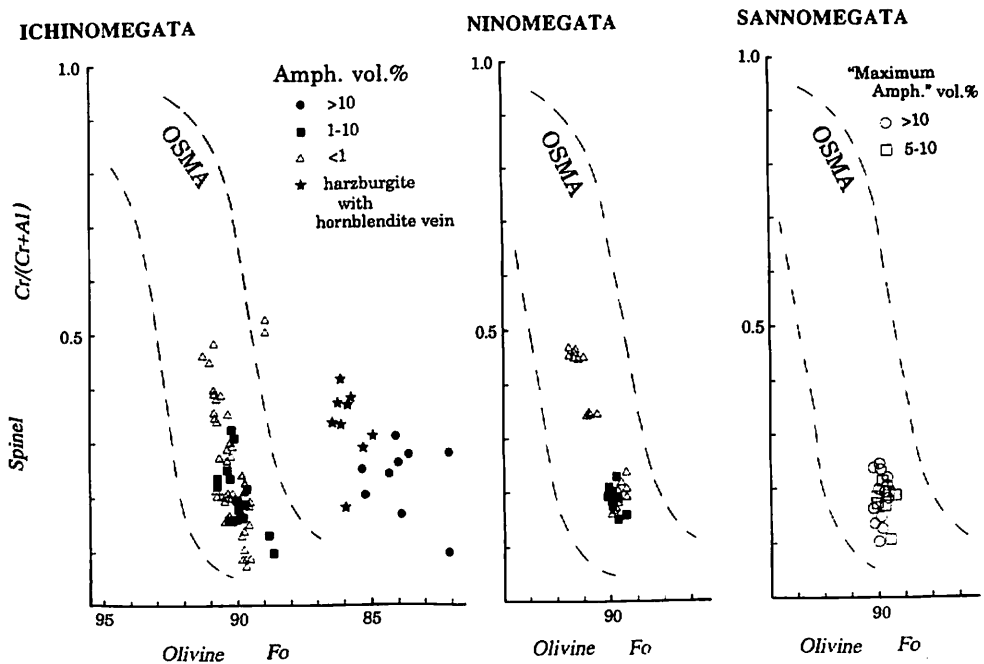


Fig. 2. Relationships between Fo of olivine and Cr# (= Cr/(Cr + Al) atomic ratio) of chromian spinel. Note that the degree of scattering of peridotite compositions decreases from Ichinomegata to Sannomegata through Ninomegata. "Maximum amphibole" is a fine-grained aggregate of pyroxenes, spinel and plagioclase with or without glass, which is possibly a decomposition product of amphibole, and its amount may show the maximum initial content of amphibole. See figs. 3 and 4 of Plate I.

hydrated harzburgites. They are harzburgite in terms of modal ratio of olivine and pyroxenes (almost free of clinopyroxene) but sometimes contain relics of spinel-pyroxene symplectite, which may indicate that they had been initially lherzolitic before hydration.

3. Mineral chemistry

Detailed mineral chemical data will be described elsewhere and a brief description will be made here. Olivine in anhydrous or slightly hydrated peridotites is Fo88-91 in composition (Fig. 2). Strongly hydrated peridotites have much more Fe-enriched (down to Fo83) olivine (Abe et al., 1992) (Fig. 2). Chromian spinel in the Ichinomegata peridotites is strongly variable in composition; Cr# (Cr/(Cr + Al) atomic ratio) varies from 0.07 to 0.53 (Fig. 2). Spinel-pyroxene symplectite and plagioclase are contained only in fertile peridotites, with spinel of Cr# < 0.25. As pointed out by Abe et al. (1992), $Fe^{3+}/(Cr + Al + Fe^{3+})$ of spinel is distinctly higher in amphibole-rich peridotites than in nearly anhydrous ones (Fig. 3). In a particular harzburgite xenolith with hornblendite selvage (I-706; figs. 1 & 2 of Plate VII) Cr# of spinel decreases towards the selvage (Abe et al., 1992).

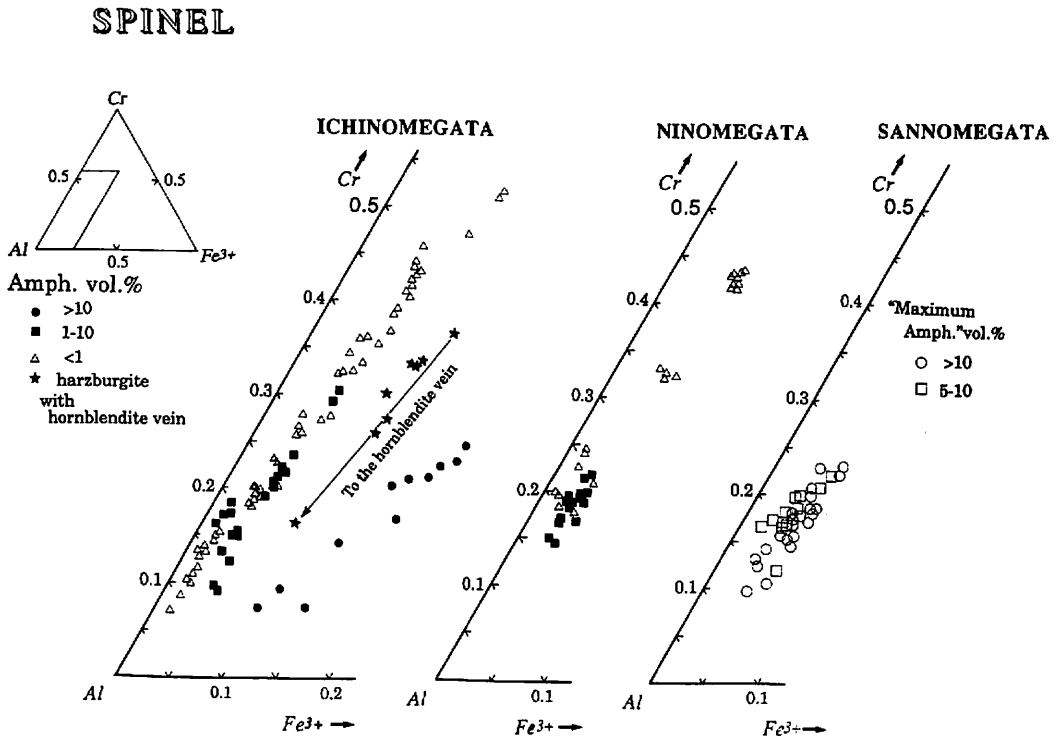


Fig. 3. Trivalent cation ratios of chromian spinel from the Megata peridotites. Note that the Fe^{3+} ratio is positively correlated with the amount of amphibole.

Pargasite generally have low TiO_2 content (< 1.6 wt. %), which is distinct from amphiboles (Ti-rich pargasite to kaersutite) in peridotites from continental rift zones and oceanic hotspots. Pargasite is slightly higher both in TiO_2 content and in $\text{K}/(\text{K} + \text{Na})$ ratio in harzburgite than in lherzolite. $\text{K}/(\text{K} + \text{Na})$ ratio is the highest in the vein-forming pargasite.

Peridotites from Sannomegata are relatively fertile and show a very narrow spread in chemistry (Figs. 2 & 3), consistent with its fertile and limited modal compositions. Peridotites from Ninomegata are intermediate in petrographical characteristics between those from Ichinomegata and Sannomegata. In other words, both mineral chemistry and petrography of peridotites become less widespread from Ichinomegata to Sannomegata through Ninomegata (Figs. 2 & 3).

4. Discussion

Variation in petrographical characteristics of peridotite xenoliths from Ichinomegata to Sannomegata may indicate a heterogeneity for both degree of hydration and degree of depletion in the upper mantle beneath Northeast Japan arc. Abundance of trails of tiny inclusions, which may be traces of fluid passage, in pyroxenites also shows a good contrast between Ichinomegata and Ninomegata (Plate IV). Hydration, which is heterogeneous horizontally, may be one of petrological characteristics of the arc mantle.

It is noteworthy that dunite or dunitic layers or patches are usually associated with pyroxenites or other pyroxene-rich rocks. The dunite appears to be a kind of depletion aureole around pyroxenites, which could be cumulates from some melt. This interpretation is basically consistent with observations of Arai and Muraoka (1992) for xenoliths from Southwest Japan that abundance of dunite and pyroxenites is positively correlated with the degree of refractoriness of associated mantle peridotites. The relatively rarity of dunite xenoliths from the Megata volcano is consistent with the high averaged fertility of the peridotite xenoliths.

Almost complete absence of chromitite is also characteristic of the Megata xenolith suite. According to Arai and Yurimoto (1993) chromitites in the upper mantle are interaction products between basaltic melt and refractory harzburgite. The absence of chromitite is consistent of the relatively fertility with the Megata peridotites.

Acknowledgements

We are very grateful to Y. Saeki, who approved our access to his sample collection and thin sections. Many people helped us to collect xenolith samples. We are especially indebted to A. Ninomiya, N. Takahashi, M. Matsuzawa, K. Taguchi, H. Watanabe and H. Jumonji for their donation of important samples used in this study. We were benefitted from advice of A. Ishiwatari and M. Okuno in SEM analysis. We greatly

appreciate E. Takahashi's encouragement.

References

- Abe, N., Arai, S. and Saeki, Y. (1992). Hydration processes in the arc mantle; petrology of the Megata peridotite xenoliths, the Northeast Japan arc. *Jour. Min. Petr. Econ. Geol.*, v. 87, p. 305-317 (in Japanese with English abstract).
- Aoki, K. (1971). Petrology of mafic inclusions from Itinome-gata, Japan. *Contrib. Mineral. Petrol.*, v. 30, p. 314-331.
- and Prinz, M. (1974). Chromian spinels in lherzolite inclusions from Itinome-gata, Japan. *Contrib. Mineral. Petrol.*, v. 18, p. 326-337.
- and Shiba, I. (1973). Pargasites in lherzolite and websterite inclusions from Itinome-gata, Japan. *Jour. Japan. Assoc. Min. Petr. Econ. Geol.*, v. 68, p. 303-310.
- Arai, S. (1986). K/Na variation in phlogopite and amphibole of upper mantle peridotites due to fractionation of the metasomatizing fluids. *Jour. Geol.*, v. 96, p. 436-444.
- (1987). Xenoliths of "cumulates" from Ichinomegata and Sannomegata, Japan. *Jour. Min. Petr. Econ. Geol.*, v. 82, p. 51-59
- (1990). Upper mantle to lower crustal materials beneath the Japan arcs. *Earth Monthly*, v. 12, p. 587-590 (in Japanese with English abstract).
- and Kobayashi, Y. (1981). Frequency of ultramafic rocks as inclusions in some alkali basalts from southwestern Japan and its bearing on the constitution of the upper mantle. *Ann. Rep. Inst. Geosci. Univ. Tsukuba*, no. 7, p. 66-69.
- and Saeki, Y. (1980). Ultramafic-mafic inclusions from Sannomegata crater, Oga Peninsula, Japan, with special reference to the petrographical difference from the Ichinomegata inclusions. *Jour. Geol. Soc. Japan*, v. 86, p. 705-708.
- and Takahashi, N. (1987). A kaersutite-bearing dunite xenolith from Ichinomegata, northeastern Japan. *Jour. Min. Petr. Econ. Geol.*, v. 82, p. 85-89 (in Japanese with English abstract).
- and Muraoka, H. (1992). Peridotite xenoliths in alkali basalts from On-yama, the Chugoku district, as a suite of fertile upper mantle peridotites beneath the Southwest Japan arc. *Jour. Min. Petr. Econ. Geol.*, v. 87, p. 240-251 (in Japanese with English abstract).
- and Yurimoto, H. (1993). Podiform chromitites as mantle-melt interaction products. *Abst. IAVCEI General Assembly, Canberra*, p. 3.
- Fujinawa, A. and Hayashi, S. (1993). Various REE characteristics of magmas erupted at Kampo volcano, Northeast Japan: Implications for genetic relations among coexisting magma suites in back-arc side volcanoes. *Jour. Min. Petr. Econ. Geol.*, v. 88, p. 205 (in Japanese).
- Horie, S. (1964). Some age data for the study on development of lakes. *Kagaku (Science), Iwanami*, v. 34, p. 98 (in Japanese).

- Katsui, Y., Yamamoto, M., Nemoto, S. and Niida, K. (1979). Genesis of calc-alkalic andesites from Oshima-Ōshima and Ichinomegata volcanoes, North Japan. *Jour. Fac. Sci., Hokkaido Univ.*, v. 19, p. 157-168.
- Ninomiya, A. and Arai, S. (1992). Harzburgite fragment in a composite xenolith from an Oshima-Ōshima andesite, the Northeast Japan arc. *Bull. Volcanol. Soc. Japan.*, v. 37, p. 269-273 (in Japanese).
- Richard, M. (1986). *Géologie et Pétrologie d'un Jalon de L'arc Taiwan-Luzon: L'île de Batan (Philippines)*. Thèse de Doctrat de L'Université de Bretagne Occidentale. 351 p. (in French with English abstract).
- Saeki, Y. (1979). *Petrographical study of xenoliths from Ichinome-gata and Sannome-gata, Akita Prefecture, Northeast Japan*. Graduation thesis, Shizuoka Univ. 81 p. (in Japanese with English abstract).
- Takahashi, E. (1980). Thermal history of lherzolite xenoliths - Petrology of lherzolite xenoliths from the Ichinomegata crater, Oga Peninsula, northeast Japan, Part I. *Geochim. Cosmochim. Acta.*, v. 44, p. 1643-1658.
- (1986). Genesis of calc-alkali andesite magma in a hydrous mantle crust boundary: petrology of lherzolite xenoliths from the Ichinomegata crater, Oga peninsula, northeast Japan, part II. *Jour. Volcanol. Geotherm. Res.*, v. 29, p. 355-395.
- Tanaka, T. and Aoki, K. (1981). Petrogenic implications of REE and Ba data on mafic and ultramafic inclusions from Itinome-gata, Japan. *Jour. Geol.*, v. 89, p. 369-390.
- Vidal, P., Dupuy, C., Maury, R. and Richard, M. (1989). Mantle metasomatism above subduction zones: Trace-element and radiogenic isotope characteristics of peridotite xenoliths from Batan Island (Philippines). *Geology*, v. 17, p. 1115-1118.

Captions for Plates

Scale bars denote 0.5 mm for photomicrographs. Sample numbers initiated by I-, N-, and S- denote the sampling locality of Ichinomegata, Ninomegata and Sannomegata, respectively.

Plate I Lherzolite

- fig. 1 Relatively fine-grained lherzolite from Ichinomegata (I-934).
- fig. 2 Photomicrograph of I-934 lherzolite. Crossed-polarized light.
- fig. 3 Photomicrograph of spinel-pyroxene symplectite (Symp) and surrounding "fine-grained aggregate" (S-1001). Plane-polarized light.
- fig. 4 Crossed-polarized light.

Plate II Harzburgite

- fig. 1 One of the largest peridotite xenoliths from the Megata volcano (I-708). Note that harzburgite is coarser-grained than lherzolite.
- fig. 2 Coarse-grained harzburgite (I-744).
- fig. 3 Photomicrograph of I-744 harzburgite. Crossed-polarized light.
- fig. 4 Photomicrograph of a seam of chromian spinel with pyroxenes in harzburgite (N-04). Plane-polarized light.

Plate III Harzburgite with porphyroclastic texture

- fig. 1 Photomicrograph of the porphyroclastic texture (N-06). Strongly kinked olivine porphyroclast surrounded by fine neoblasts. Crossed-polarized light.
- fig. 2 Photomicrograph of kinked orthopyroxene porphyroclasts surrounded by olivine neoblasts (N-06).
- fig. 3 Photomicrograph of spinel inclusions in pyroxenes and olivine (N-06). Relatively small clinopyroxene porphyroclast in the center contains lamellar spinel, whereas neoblasts of olivine and orthopyroxene have granular spinel inclusions. Plane-polarized light.
- fig. 4 Photomicrograph of kinked olivine porphyroclasts in harzburgite from Ichinomegata (I-743). Crossed-polarized light.

Plate IV Websterites

- fig. 1 Photograph of a thin section of websterite from Ichinomegata (I-778). Note that dunitic patches (or seams) and numerous crisscrossing trails of fine inclusions which we interpreted traces of fluid passage.
- fig. 2 Photomicrograph of I-778 websterite. Note the inclusion trails (between arrow heads) and amphibole on grain boundaries of pyroxenes. Plane-polarized light.
- fig. 3 Photograph of a thin section of websterite from Ninomegata (N-12). Note the almost absence of inclusion trails in contrast to the Ichinomegata ones (see above).
- fig. 4 Photomicrograph of N-12 websterite. Pyroxenes are almost free of inclusion trails (compare to fig. 2) and small amount of amphibole is observed on grain boundaries. Plane-polarized light.

Plate V Pyroxenites

- fig. 1 Thin section photograph of websterite (I-775). Note relatively thick trails of inclusions some of which are crisscrossing.
- fig. 2 Photomicrograph of a thick trail of inclusions (I-775). Some of the inclusions are composed of chromian spinel and amphibole (Am, brown) is sometimes formed along the trail. Plane-polarized light.
- fig. 3 Photomicrograph of amphibole vein in clinopyroxenite (I-767). Note that thin amphibole veinlets branch away along grain boundaries of pyroxene. Plane-polarized light.
- fig. 4 Photomicrograph of orthopyroxenite (I-770), which is coarser-grained than websterites and clinopyroxenites. A trail of fine inclusions and amphibole runs from upper right to lower left.

Plate VI Modes of occurrence of amphibole

- fig. 1 Pargasite (Am) around chromian spinel (Sp) in strongly hydrated peridotite (I-014). Note the deep color of spinel which is high in Fe^{3+} . Plane-polarized light.

fig. 2 Pargasite (Am) replacing spinel-pyroxene symplectite (Symp) (I-651). Note the partly digested symplectite in pargasite. Plane-polarized light.

fig. 3 Pargasite (Am) replacing pyroxenes of symplectite (I-738). Plane-polarized light.

fig. 4 Pargasite (Am) formed along the grain boundaries of pyroxenes (I-738). Plane-polarized light.

Plate VII Composite xenoliths

fig. 1 Harzburgite xenolith with hornblendite selvages (upper and lower margins, dark) (I-706). This sample was described in detail by Abe et al. (1992).

fig. 2 Photomicrograph of the hornblendite selvage (Am) on harzburgite (harz) with intervening orthopyroxenite (Opx). The boundaries are highlighted by thick lines. Plane-polarized light.

fig. 3 Thin section photograph of lherzolite with hornblendite veins (dark) (N-05).

fig. 4 Photomicrograph of lherzolite cut by a hornblendite vein (N-05). Plane-polarized light.

Plate VIII Hornblendite with lherzolite selvage (I-933)

fig. 1 Lherzolite selvage on fine-grained hornblendite.

fig. 2 Photomicrograph of the lherzolite selvage (left) on hornblendite. The boundary between hornblendite and lherzolite is not sharp. Note the spinel-pyroxene symplectite near the boundary. Plane-polarized light.

fig. 3 Photomicrograph of hornblendite. Hornblende often has fine inclusions of spinel and other minerals. Light-colored mineral is orthopyroxene. Plane-polarized light.

Plate IX Composite xenoliths

fig. 1 Dunite and pyroxene-rich lherzolite (or olivine websterite) with intervening websterite (arrow) (I-883). Note that small dunitic patches are present on the right side of the websterite layer.

fig. 2 Photomicrograph of websterite (left) and dunitic patch (right) (I-883). In the websterite layer amphibole is abundant and clinopyroxene is enriched with spinel lamellae and other inclusions. Plane-polarized light.

fig. 3 Pyroxene-rich lherzolite (or olivine websterite) with dunite layer (between arrow heads) (I-873).

fig. 4 Photomicrograph of pyroxene-rich lherzolite of fig. 3 (I-873). Large amount of amphibole is formed, replacing pyroxenes. Plane-polarized light.

Plate X Fine-grained lherzolite with clinopyroxenite (or gabbro) vein (I-716)

fig. 1 Natural surface of the lherzolite (I-716). Note that coarse plagioclase is formed in the center of clinopyroxenite vein (arrow).

fig. 2 Sawed surface perpendicular to the clinopyroxenite vein of fig. 1. Plagioclase does not appear on this surface.

fig. 3 Thin section of the sawed piece (fig. 2). Dunitic patches and layers are found in around the clinopyroxenite vein. Note that the clinopyroxenite vein cuts the lineation of the lherzolite (see fig. 4).

fig. 4 Explanation of figs. 2 and 3.

Plate XI Composite xenoliths

fig. 1 Layered dunite (upper left), wehrlite and clinopyroxenite (lower right) (I-734). Dunite is coarse-grained, wehrlite is fine-grained and clinopyroxenite (dark) is relatively coarse-grained.

fig. 2 Photograph of thin section of websterite/wehrlite composite xenolith (I-765). Websterite (lower) is coarser-grained than wehrlite (upper). Inclusion trails are abundant in the websterite part but disappear in a few clinopyroxene grains across the boundary into the wehrlite part.

fig. 3 Photomicrograph of the gabbro (upper)/websterite (lower) boundary in a composite xenolith (I-745). Upper right is a dunite patch on the boundary. In the gabbro part spinel-pyroxene symplectite is prominent between plagioclase and olivine. In the websterite part amphibole is abundant in grain boundaries and in orthopyroxene, replacing clinopyroxene lamellae. Plane-polarized light.

fig. 4 Crossed-polarized light (I-745).

Plate XII Composite xenoliths

fig. 1 Lherzolite with a pyroxene-rich layer (or vein; arrow) (I-735).

figs. 2 and 3 Photomicrograph of the pyroxene-rich vein of fig. 1 (I-735). The inclusion trail (between arrow heads) with amphibole is frequently found. Plane-polarized light.

fig. 4 Lherzolite with pyroxene-rich layers (or Heterogeneous lherzolite) (I-777).

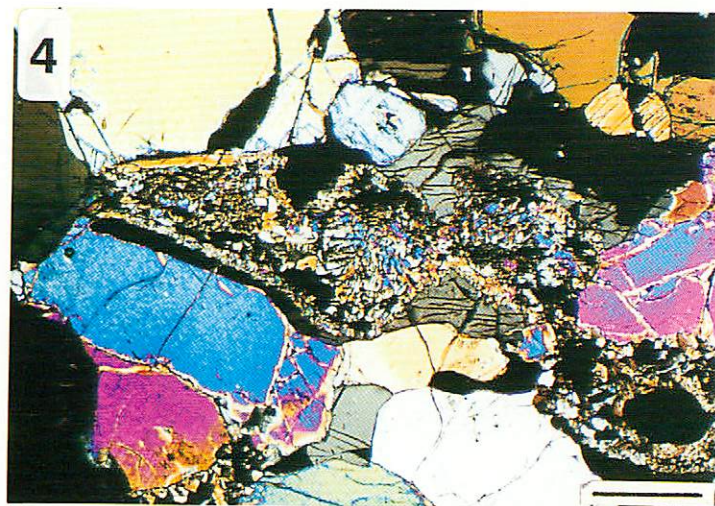
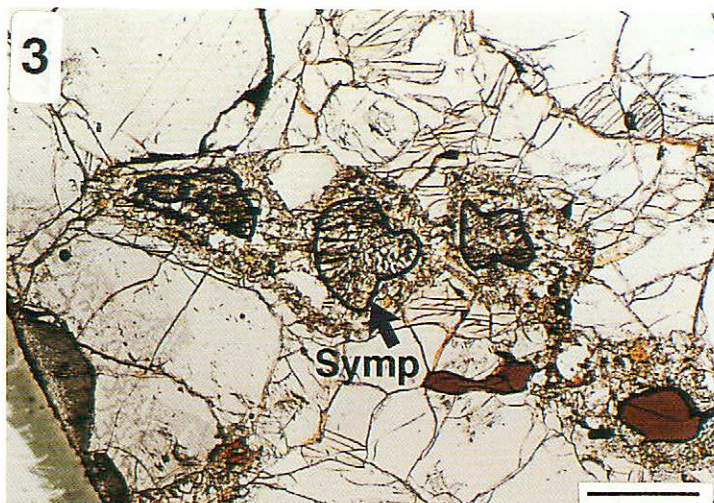
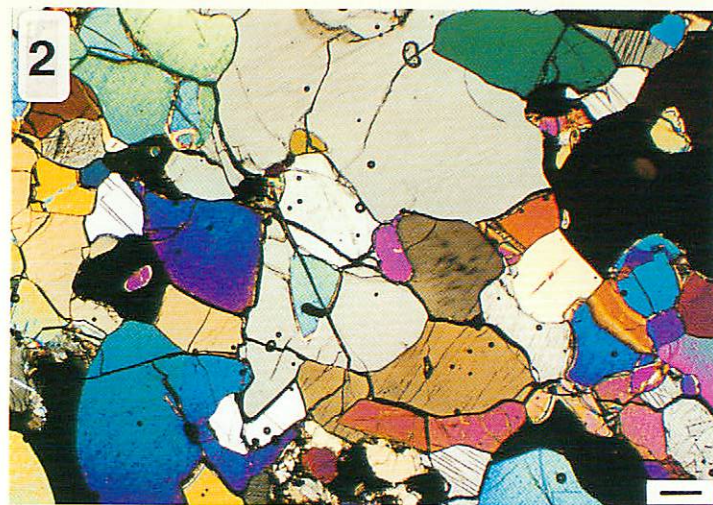


Plate II

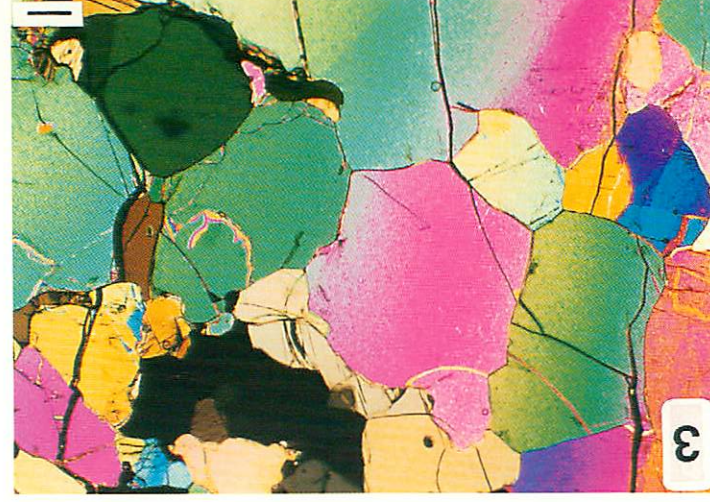


Plate III

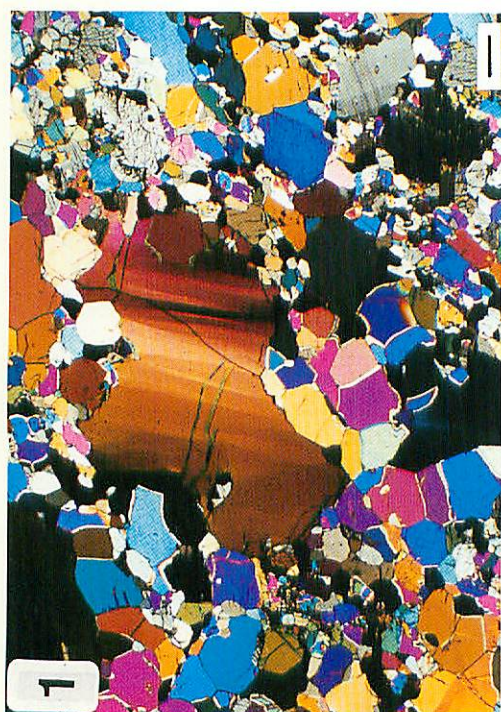
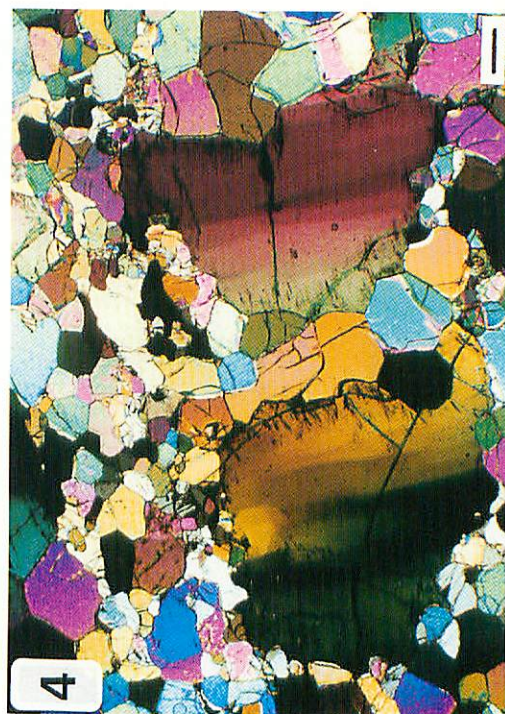
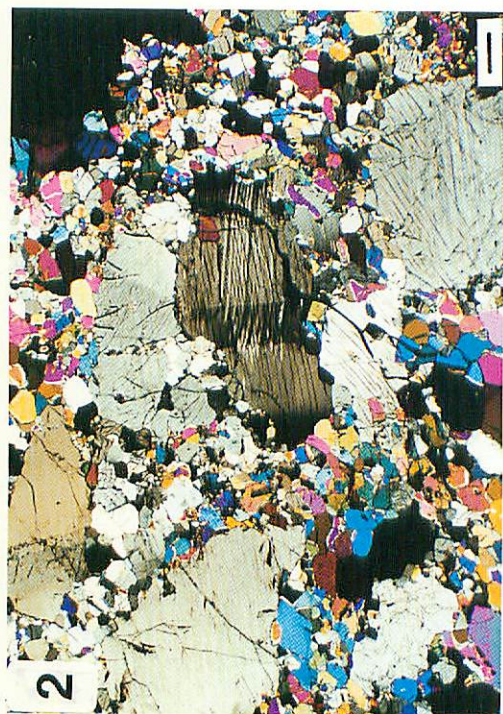


Plate IV



Plate V

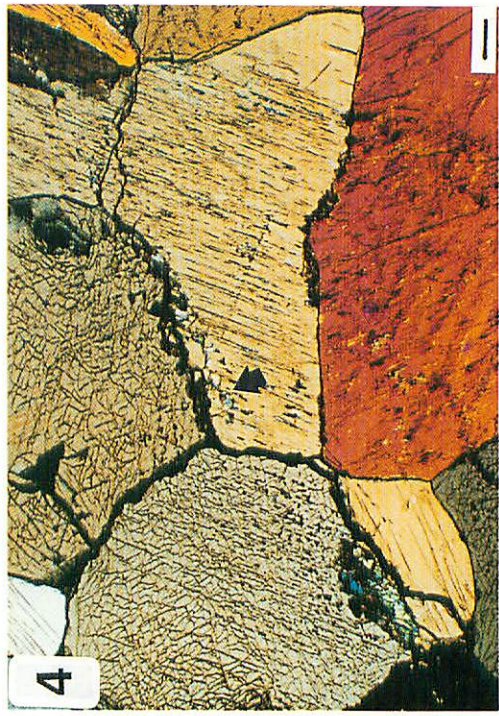


Plate VI

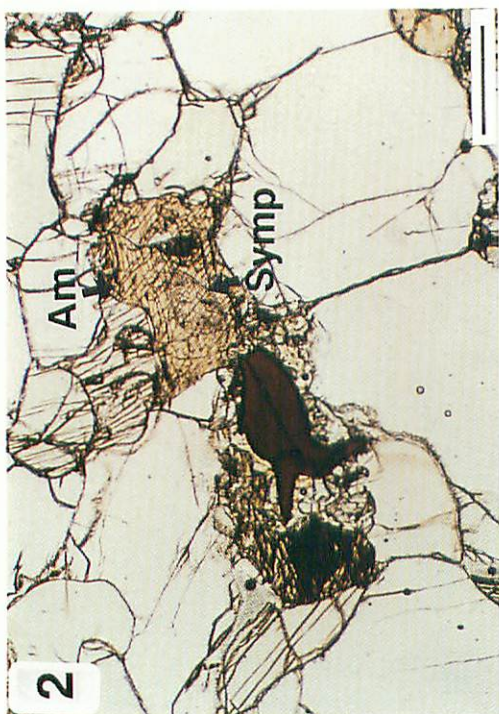


Plate VII

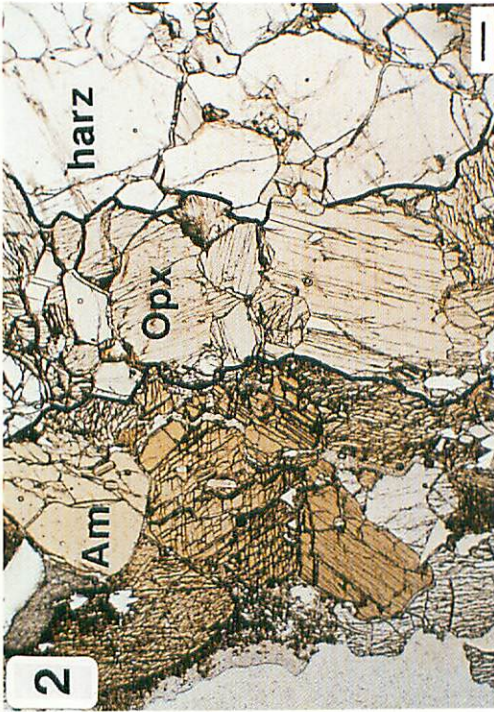


Plate VIII

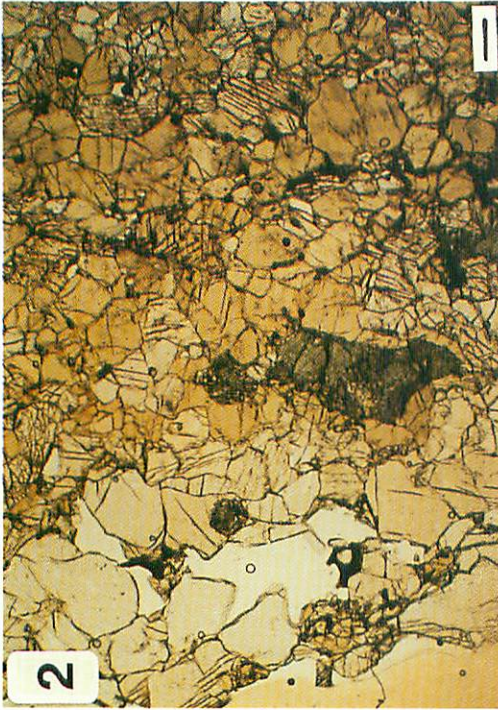


Plate IX

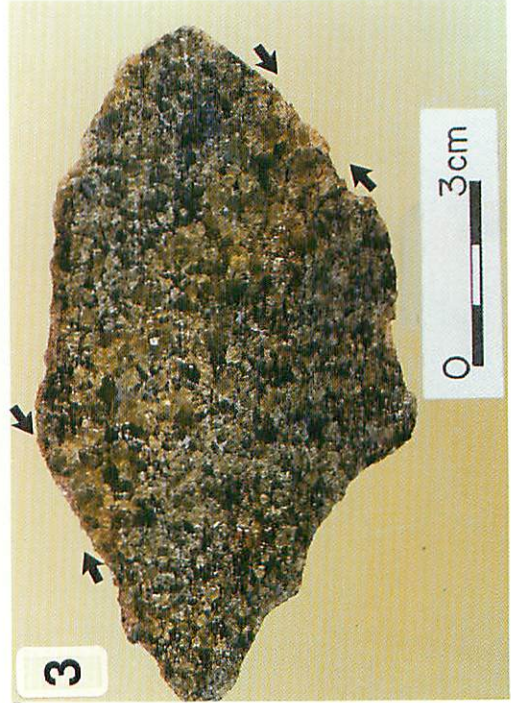
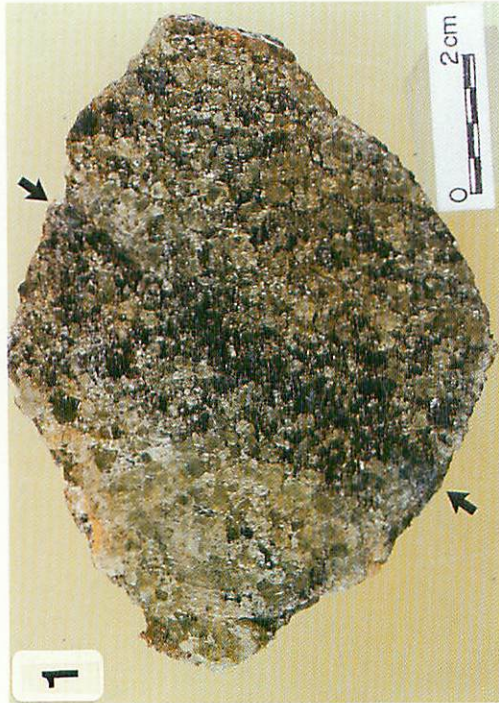


Plate X

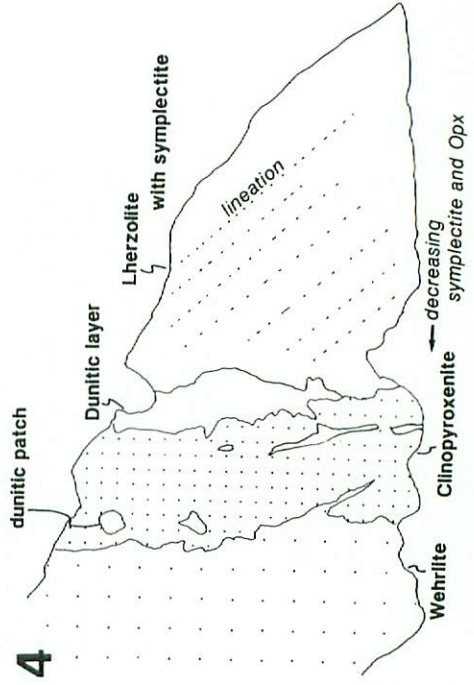
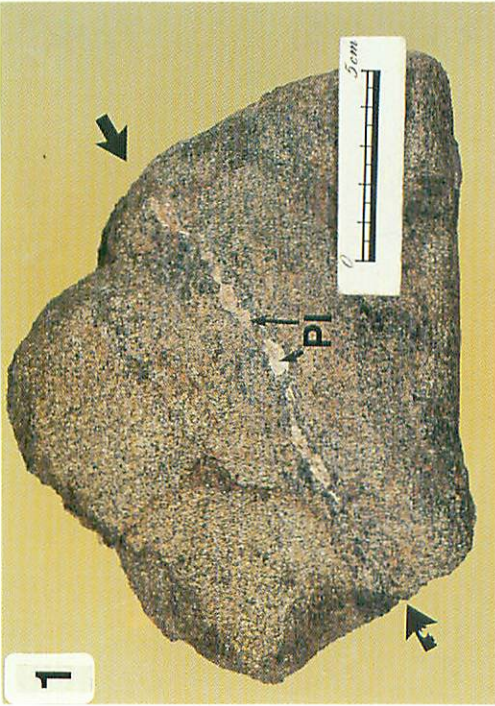


Plate XI

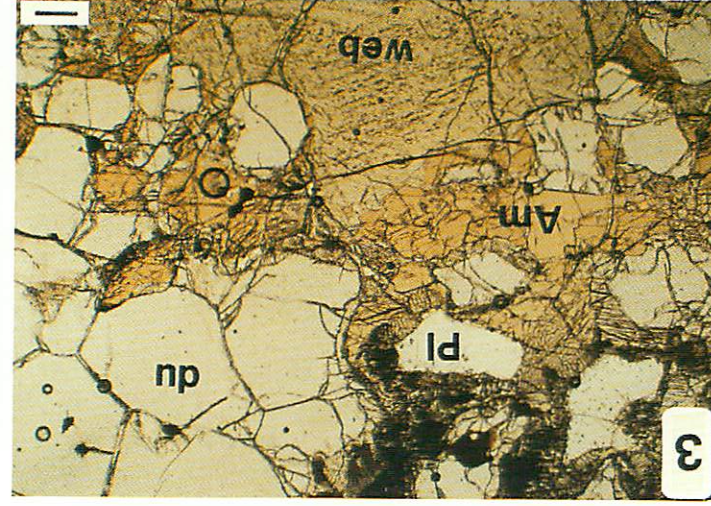
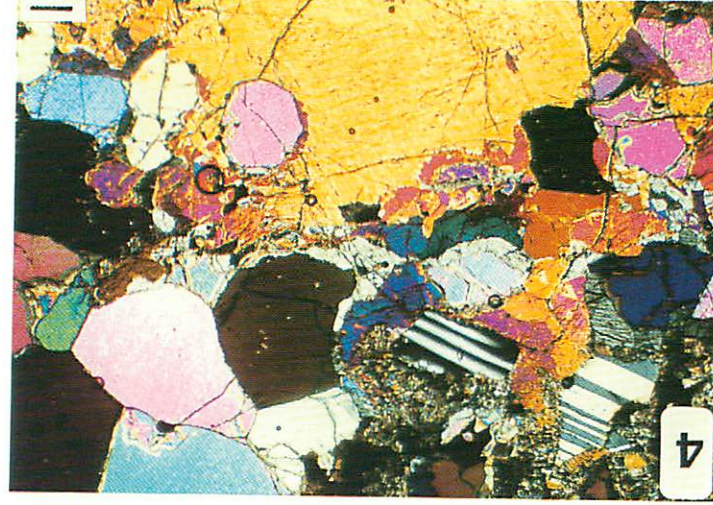
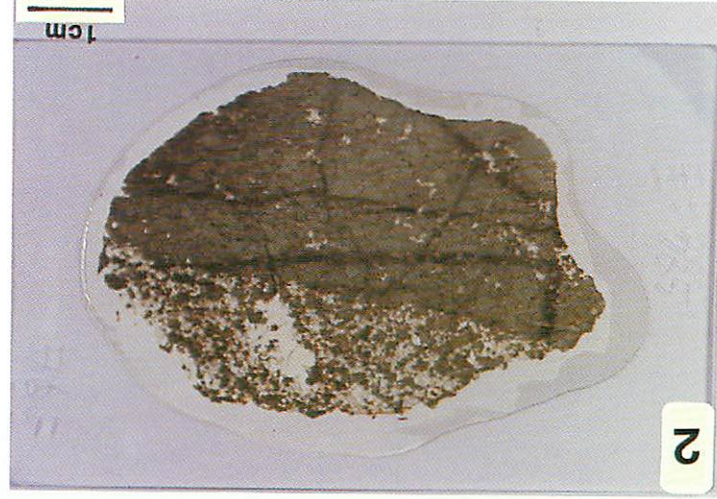


Plate XII

